A Numerical Method for the Calculation of Nonlinear, Unsteady Lifting Potential Flow Problems

R. HARIJONO DJOJODIHARDJO* AND SHEILA E. WIDNALL†
Massachusetts Institute of Technology, Cambridge, Mass.

A numerical method is developed for attacking lifting problems of a general three-dimensional wing executing an arbitrary motion in a potential flow. The formulation of the problem is exact in the sense that the boundary conditions are satisfied on the surface of the wing and the geometry of the time-dependent wake is predicted. The problem is then governed by a Fredholm integral equation of the first kind which relates the velocity potential doublet distribution to the normal velocity on the surface of the wing, subject to the Kutta condition of smooth flow off the trailing edge and the condition that the wake cannot sustain any pressure difference. The solution of the integral equation is obtained in a step-by-step fashion, and the appearing surface integrals are evaluated by employing a discrete set of approximate surface elements and an assumption of the doublet distribution over the element which is based on a formal expansion of the velocity influence coefficient. Verification of the method is made by comparison with solutions of classical problems. To demonstrate its utility, the method is applied to obtain the airloads due to transient motion of wings with simple planforms. The nonlinear effects due to the wake, aspect ratio, and thickness are discussed. Results of these calculations indicate that the present method can be applied to treat more complicated geometries and motion to obtain accurate and efficient prediction of the airloads.

Nomenclature

$A;A_{ij}$ = area of the surface element; matrix of velocity influence coefficient
B_i = total apparent downwash velocity
C_{ij} = velocity potential influence coefficient
C_L,C_M; c_l,c_m = lift and moment coefficients; sectional or two-dimensional lift and moment coefficients
c = half-chord
$\mathbf{i},\mathbf{j},\mathbf{k}$ = unit vectors in the x, y, and z directions
K_v,K_{v2} = velocity kernel functions
$K_{v_x},K_{v_y},K_{v_{xx}}$, $K_{v_{xy}},K_{v_{yy}}$ = first- and second-order derivatives of K_v
M_x = area moment about the x axis
$\mathbf{n},\boldsymbol{\nu}$; n = unit normal vectors; normal coordinate
N,NC,NS = total number of surface elements, number of elements along the chord, and number of elements along the semispan
$\mathbf{Q}$ = velocity vector at a field point
R = $|\mathbf{x} - \boldsymbol{\xi}|$ = scalar distance between a field and a source point
$S(x,t)$ = the surface of the wing
s = distance travelled by the wing in half-chord; chordwise coordinate along the surface
t; Δt = dimensionless time or time; time increment
$U(t)$; U_o = freestream velocity; a reference velocity
$W(\mathbf{x},t)$ = the surface of the wake
$\mathbf{x},\boldsymbol{\xi}$;x,y,z = coordinate vector of a point; its components
α = angle of incidence
Γ = vortex strength, circulation
θ = angle
σ; σ_x,σ_{xx} = doublet strength; its derivatives
ϕ = velocity potential

Subscripts

o = centroid of a surface element
i,j,k = dummy indices; refer to element i, j, or k
x,y,z = refer to the x, y, and z directions
l = lower surface
u = upper surface

Superscripts

s = step doublet distribution or the surface of the wing
w = surface of the wake

Presented as Paper 69-23 at the AIAA 7th Aerospace Sciences Meeting, New York, January 20–22, 1969; submitted October 24, 1968; revision received April 7, 1969. This research was supported by the U.S. Army Research Office, Durham, N. C., under Contract DA-31-124-ARO-D-471. The authors would like to thank H. Ashley, of Stanford University, for suggesting the problem and for valuable suggestions in the early part of this work, and M. T. Landahl, of the Royal Institute of Technology, Stockholm, Sweden, for many stimulating discussions. The computation was performed at the Massachusetts Institute of Technology Information Processes Service Center.

* Research Assistant, Aeroelastic and Structures Research Laboratory, Department of Aeronautics and Astronautics; now Lecturer, Bandung Institute of Technology, Bandung, Indonesia.

† Assistant Professor of Aeronautics and Astronautics. Member AIAA.

I. Introduction

THE need for a more rigorous approach to the treatment of the three-dimensional flow problems involving complex motions and flow geometries derives from recent progress in V/STOL aircraft and hydrofoil craft technology. Many basic approximations inherent in classical aerodynamic theory such as the linearized boundary conditions, small perturbation velocities, and the concept of planar and rigid wake in the projected plane of the wing need careful examination when the downwash velocity associated with the generation of lift is large compared with the flight velocity. Experimental results by Greidanus, van de Vooren and Bergh,[1] Ransleben and Abramsom,[2] and Spurck[3] indicate discrepancies in the forces and moments from those predicted by linearized theories, which are attributable to the thickness of the airfoil and the viscosity of the flow.

Before any theory that accounts for the effect of viscosity may be developed, it is necessary to have available methods for predicting the pressure distribution on bodies of arbitrary geometries which execute arbitrary motions. Refinements of the linearized two-dimensional unsteady-potential flow theory have been suggested by Küssner and von Gorup,[4] Hewson-Browne,[5] van de Vooren and van de Vel,[6] Giesing,[7]

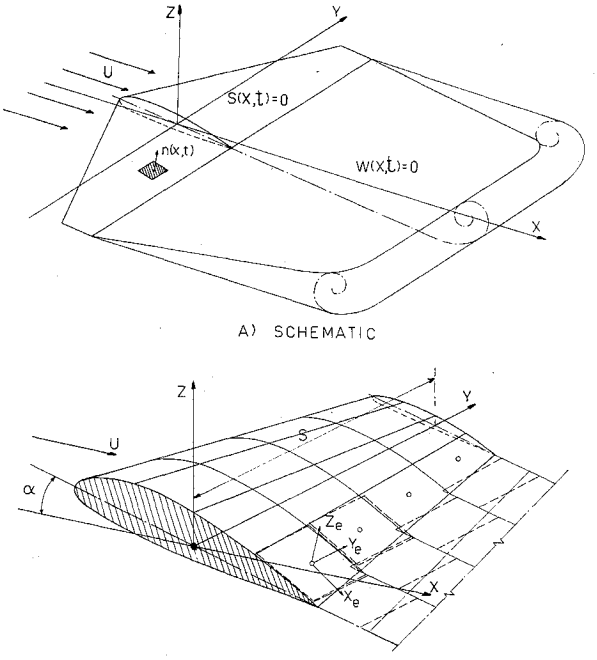

Fig. 1 Lifting system configuration.

and Chen and Wirtz.[8] Although rapid progress has been achieved in the linearized lifting surface theory for planar and nonplanar configurations in steady and unsteady flows, as is well summarized in review papers by Ashley, Widnall, and Landahl,[9] and Landahl and Stark,[10] comparatively less attention has been devoted to the case of the deforming wake and thickness effects in the more significant three-dimensional situations. Attempts to account for the deforming unsteady wake have been made in the calculation of helicopter rotor airloads, such as the works of Miller,[11,12] which involve a combined analytical and numerical procedure involving lifting line and lifting surface approximations.

The progress in high-speed digital computer technology has made possible a numerical approach with a more realistic flow model, an approach which may be termed exact in the sense that true boundary locations are accounted for and the exact solution is attained uniformly as some computation network is refined. Such an approach has been suggested by Ashley[13] and Ashley, Widnall, and Landahl[9] to account for the unsteady distorted wake, thickness, and flow geometry. The potentialities of purely numerical approaches have been demonstrated by several investigators. Hess and Smith[14] developed a very general method for calculating the nonlifting potential flow about arbitrary bodies. Giesing[7] developed a method for calculating the lifting two-dimensional flow about airfoils of arbitrary geometries and Rubbert et al.[15] developed a method to calculate the steady lifting flow about a fan-in-wing configuration including boundary-layer effects.

Obviously a numerical method to solve the unsteady, nonlinear potential flow problems associated with a wing of arbitrary geometry executing arbitrary motion should now be developed. With the foregoing in mind, the objectives of the present work can be enunciated in three parts: 1) to perform an exact numerical analysis for calculating the unsteady airloads and for predicting the geometry of the wake, 2) to verify the method through comparison with classical solutions, and 3) to apply the method to some unsteady (transient) problems and to investigate the nonlinear effects due to the deforming wake (hence the time history of the motion), the effects of thickness, and the effects of three-dimensionality of the flowfield.

II. Formulation of the Problem

Consider a lifting system configuration consisting of a three-dimensional body of arbitrary geometry which executes an arbitrary translation in an incompressible ideal fluid, as depicted in Fig. 1a. Let the surface of the lifting body be represented by

$$S(\mathbf{x},t) = 0 \tag{1}$$

and the wake following the body be defined by a surface of velocity discontinuity given by

$$W(\mathbf{x},t) = 0 \tag{2}$$

which is of zero thickness. The velocity potential for this flow then satisfies Laplace's equation, and is subject to the following boundary conditions: 1) quiescent fluid at infinity, 2) the kinematical flow tangency condition, which states that the fluid and the surface with which contact is maintained must have the same normal velocity, 3) the Kutta-Joukowski condition of smooth flow off the trailing edge, and 4) the dynamical condition of zero pressure discontinuity across the wake sheet. These conditions are sufficient to insure the existence of a unique velocity potential. The problem posed would be to find the velocity potential and the wake geometry for a specified wing in unsteady motion.

For convenience, the coordinate frame of reference is fixed on the body. Further, all quantities are rendered dimensionless by division with appropriate characteristic quantities such as chord length $2c$, reference velocity U_o, or a combination of both. By use of Green's theorem, it can be shown[13,16] that the velocity potential on the surfaces S and W and the region external to them is given by

$$\phi(\mathbf{x},t) = \frac{1}{4\pi}\iint_S \sigma(\xi,t)\frac{\partial}{\partial\nu(\xi,t)}\left[\frac{1}{R(\mathbf{x},\xi,t)}\right]dS + \frac{1}{4\pi}\iint_{W_u} \Delta\phi_w(\xi,t)\frac{\partial}{\partial\nu(\xi,t)}\left[\frac{1}{R(\mathbf{x},\xi,t)}\right]dS \tag{3}$$

where σ is the potential doublet strength over the entire surface S and $\Delta\phi_w$ is the doublet strength over the surface W, which is equal to the velocity potential discontinuity there. The first boundary condition has been incorporated in Eq. (3). ν is the outward normal at the source point (ξ,t), and $R = |\mathbf{x} - \xi|$ where $P(\mathbf{x},t)$ is a field point. For $P(\mathbf{x},t)$ on S or W, the first or second integral in Eq. (3), respectively, is singular, but proper evaluation can be made by a limiting process.

The velocity at any field point is given by

$$\mathbf{Q} = \mathbf{i}U/U_o + \nabla\phi \tag{4}$$

where U is the freestream velocity, conveniently aligned with the x axis. The kinematical boundary condition on the surface of the body is given by

$$\frac{dS}{dt} = \frac{\partial S}{\partial t} + \left(\frac{U}{U_o}\mathbf{i} + \nabla\phi\right)\cdot\nabla S = 0 \text{ on } S(\mathbf{x},t) = 0 \tag{5}$$

Noting that $\nabla S/|\nabla S| = \mathbf{n}$ and $(1/|\nabla S|)(\partial S/\partial t) = \partial n/\partial t$, the dimensionless velocity of S normal to itself, Eq. (5) can be rearranged to yield

$$\frac{\partial\phi}{\partial n} = -\frac{U}{U_o}\mathbf{i}\cdot\mathbf{n} - \frac{\partial n}{\partial t} \text{ on } S(\mathbf{x},t) = 0 \tag{6}$$

Substituting Eq. (3) into Eq. (6) and rearranging, we obtain

$$\frac{1}{4\pi}\iint_S \sigma(\xi,t)\frac{\partial^2}{\partial n\partial\nu}\left[\frac{1}{R(\mathbf{x},\xi,t)}\right]dS = -\frac{U}{U_o}\mathbf{i}\cdot\mathbf{n} - \frac{\partial n}{\partial t} - \frac{1}{4\pi}\iint_{W_u}\Delta\phi_w\frac{\partial^2}{\partial n\partial\nu}\left[\frac{1}{R(\mathbf{x},\xi,t)}\right]dS \tag{7}$$

which is a singular Fredholm integral equation of the first

kind and comprises the ensuing equation for the velocity potential field of the flow. Since the integral involves a single kernel, the coefficient of the doublet strength of the integral, evaluation should be made in the principal value sense.[17,18]

Dynamical Condition Governing the Wake

From momentum consideration, the force acting on the lifting configuration consisting of S and W is given by

$$F = \frac{D}{Dt}\left[\iint_S \phi \mathbf{n} dS + \iint_{W_u} \Delta\phi_w \mathbf{n} dS\right] \tag{8}$$

Since the wake cannot sustain any pressure difference across it,

$$(D/Dt) \iint_{W^u} \Delta\phi_w \mathbf{n} dS = 0$$

which can be further reduced to

$$(D/Dt)\{\Delta\phi_w\} = 0 \tag{9}$$

That is, once a fluid particle in the wake is imparted a doublet strength $\Delta\phi_w$, this value remains constant as it is convected downstream. This condition is equivalent to Kelvin's theorem.

The Kutta-Joukowski Condition and the Generation of the Wake

A general statement known as the extended Kutta-Joukowski condition implies that the rear dividing streamline leaves the airfoil at the trailing edge. Its tangent at the trailing edge, in general, passes through the interior of the airfoil.[19] The Kutta-Joukowski condition was originally applied in a two-dimensional steady flow in order to obtain a finite velocity at the trailing edge, and as a consequence, the flowfield is uniquely determined. This hypothesis implicitly accounts for the viscous effects otherwise neglected in inviscid theory. In the classical unsteady flow calculations, the Kutta-Joukowski condition is applied at any instant[20] or for each set of wake vortex and its image inside the circle (in the circle plane).[21]

In the present inviscid approach for a three-dimensional unsteady flow, the foregoing general statement is applied. Since the wake then emerges from the trailing edge, the dynamical condition (9) governing the wake also applies at the trailing edge. This condition can be shown[16] to be equivalent to the finiteness of the velocity at the trailing edge, provided no discontinuous motion of the airfoil takes place. As another consequence, $\Delta\phi$ is continuous through the trailing edge, as also mentioned in Ref. 13. For a thick body with a sharp trailing edge, $\Delta\phi$ at the trailing edge can be defined in the limiting sense as the difference between the values of the doublet strengths at the upper and lower surfaces there; thus

$$\sigma_{TE} = \lim_{x \to TE} (\sigma_u - \sigma_l) \tag{10}$$

The velocity of the wake shedding at the trailing edge is determined by

$$Q_{TE} = (U/U_o)\mathbf{i} + (\nabla\phi)_m \tag{11}$$

where $(\nabla\phi)_m = \frac{1}{2}[(\nabla\phi)_u + (\nabla\phi)_l]$.

Pressure, Forces, and Moment

From the Bernoulli equation and the use of expression (4), the pressure coefficient can be written as

$$c_p = -2\left(\frac{U}{U_o}\right)^2\left(\frac{x}{U_o}\frac{\partial U}{\partial t} + \frac{\partial\phi}{\partial t}\right) - \left(\mathbf{i}\frac{U}{U_o}\cdot 2\nabla\phi + \nabla\phi\cdot\nabla\phi\right) \tag{12}$$

For a constant freestream velocity, $U = U_o$ and Eq. (12) is further simplified.

The lift, drag, and moment coefficients can be obtained by the usual procedure of integrating the vertical and horizontal components and the moments of these components with respect to the origin, respectively, over the surface of the wing and appropriately divising by the largest projected area of the wing or by the product of this area with the root chord of the wing.

An alternative formula can be derived to calculate the lift, employing the velocity potential distribution directly. Taking the vertical component of Eq. (8) and the use of expression (4), the lift on the wing can be shown to be

$$C_L = \frac{1}{A}\left[\frac{\partial}{\partial t}\iint_S \phi \mathbf{n}\cdot\mathbf{k} dS + \frac{U}{U_o}\iint_S \frac{\partial\Phi}{\partial s}(\mathbf{n}\cdot\mathbf{k})^2 dS\right] \tag{13}$$

which can be evaluated by numerical means upon knowing the values of ϕ at any point on the surface S. Since it is not necessary to calculate the pressure coefficients, rapid computation results. Similar formulas can be derived for the drag and moment coefficients. The first integral on the right-hand side of Eq. (12) represents the unsteady part, and the second has the same form as in steady flow.

To obtain the starting lift for impulsive motion, for which the accuracy of a numerical differentiation is difficult to assess, an alternative method is suggested below. For this purpose, we could write

$$\phi(\mathbf{x}_j,t) = PO\{B(\mathbf{x}_i,t)\} \tag{14}$$

in the absence of the wake. The notation PO is the potential operator as employed by Giesing,[7] which will be elaborated in Sec. III. The starting lift is given by

$$C_{Lm} = \frac{1}{A}\frac{\partial}{\partial t}\iint_S \phi dS = \frac{1}{A}\iint_S \frac{\partial\phi}{\partial t} dS \tag{15}$$

Since the potential operator as implied in (14) is a linear one, then

$$\frac{\partial\phi(\mathbf{x}_j)}{\partial t} = \frac{\partial}{\partial t}[PO\{B(\mathbf{x}_j,t)\}] = PO\left\{\frac{\partial}{\partial t}B(\mathbf{x}_j,t)\right\} \tag{16}$$

which should be used in Eq. (15). Equation (16) can be evaluated according to a numerical scheme developed subsequently to evaluate ϕ in (14). Hence this procedure is similar to solving the boundary value problem associated with the flow situation at the starting instant, where the boundary condition of flow tangency at the surface of the body should be replaced by its time derivative. For an impulsively started elliptical planform, this procedure yields a result that agrees with that of R. T. Jones.[22] This procedure can also be employed to calculate the unsteady term due to discontinuous motion.

III. Method of Solution

The problem of obtaining the velocity potential field of the ensuing flow has been reduced to an integral equation which relates the velocity potential doublet distribution on the surface of the lifting system configuration to the normal induced velocity variation on the surface of the wing, as expressed by Eq. (7), and which is subject to the dynamical condition (9) on the wake sheet and the Kutta-Joukowski condition of smooth flow off the trailing edge. The velocity potential field is then determined from Eq. (3). The integral equation (7) is nonlinear in the sense that solutions for various flows cannot be superimposed. The nonlinearity arises from the fact that the doublet distribution on the wake as well as the wake location are implicitly dependent on the doublet distribution on the surface of the wing, since the location of the wake sheet at any instant is a function of the previous velocity potential field. In addition, the normal

component of the freestream velocity to the surface of the wing—the first term on the right-hand side of Eq. (7)—is exact rather than linearized as in most lifting surface theories.

To solve Eq. (7), two problems immediately arise: 1) the determination of the geometry of the wake $W(x,t)$, and 2) the solution of the integral equation for known right-hand-side terms. One possible approach is to employ a step-by-step procedure, so that at each step, with the aid of condition (9) and the Kutta-Joukowski condition, the terms on the right-hand side of (7) would be known. Solution of the integral equation then becomes a matter of numerical analysis.

Step-by-Step Procedure

At the initial instant of motion, no wake exists, and hence no wake term appears on the right-hand side of Eq. (7) and the remaining equation can be solved for $\sigma(\mathbf{x},t)$. To solve for the situation at successive instants, an assumption could be made regarding the variation of the velocity field during a small time increment Δt. Then the location of a wake element emerging off the trailing edge can be predicted from the following set of equations:

$$\mathbf{x}_w(t_o,t) = \int_{t_i}^{t} Q(\mathbf{x},t_l)dt_k + \mathbf{x}_w(t_o t_i) \tag{17}$$

$$Q(\mathbf{x},t) = \frac{U}{U_o}\,\mathbf{i} + \nabla_s \phi_{wm}(\mathbf{x},t) + \mathbf{n}\,\frac{\partial \phi(\mathbf{x},t)}{\partial n} \tag{18}$$

where ϕ_{wm} is the mean velocity potential on the wake sheet and the subscript s on the gradient operator indicates that the operation is performed along the wake surface, and where

$$\frac{\partial \phi(\mathbf{x},t)}{\partial n} = \frac{1}{4\pi}\oint\!\!\oint_S \sigma(\xi,t)\,\frac{\partial^2}{\partial n(\mathbf{x},t)\,\partial \nu(\xi,t)}\left[\frac{1}{R(\mathbf{x},\xi,t)}\right]dS + \frac{1}{4\pi}\iint_W \Delta\phi_w(\xi,t)\,\frac{\partial^2}{\partial n(\mathbf{x},t)\,\partial \nu(\xi,t)}\left[\frac{1}{R(\mathbf{x},\xi,t)}\right]dS \tag{19}$$

Obviously, ϕ_{wm} can be defined and Eq. (19) can be used after the wake has emerged. The wake elements carry with them the values of $\Delta\phi_w$ imparted at the instant of shedding, which is numerically set equal to the velocity potential jump at the trailing edge at that instant [Eq. (10)]. Each value of $\Delta\phi_w$ is fixed for any wake element of fixed identity, according to (9). Setting t_o equal to the instant of shedding for each wake element, then $\mathbf{x}_w(t_o,t_i) = \mathbf{x}_{TE}$. Hence, at each time step, all terms on the right-hand side of Eq. (7) are again known. By repeated use of such procedure, the transient loading of any motion can be obtained. The steady or periodic loading is obtained after all transient effects subside. Clearly, such a procedure is best suited for solving transient problems.

Numerical Method

It is convenient to cast the integral equation (7) into the following form:

$$[A_{ij}]\{\sigma_i\} = \{B_j\} - [A_{kj}{}^w]\{\Delta\phi_{wk}\} \tag{20}$$

incorporating a discrete set of surface elements to represent the lifting surface configuration. Here

$$A_{ij} = \frac{1}{4\pi}\iint_{\text{el } i}\frac{\sigma(\xi,t)}{\sigma(\mathbf{x}_{oi},t)}\,\frac{\partial^2}{\partial n(\mathbf{x},t)\partial \nu(\xi,t)}\left[\frac{1}{R(\mathbf{x},\xi,t)}\right]dS \tag{21}$$

is the velocity influence coefficient, representing the velocity induced at a field point $P(\mathbf{x}_j,t)$ due to doublet distribution over the surface element i and $\mathbf{x}_{oi}$ is a representative point on the element. Further,

$$B_j = -\frac{U}{U_o}\,\mathbf{i}\cdot\mathbf{n}(\mathbf{x}_j,t) - \frac{\partial n(\mathbf{x}_i,t)}{\partial t} \tag{22}$$

The solution can be obtained by inverting the matrix of influence coefficient A; thus

$$\{\sigma\} = [A]^{-1}\{B'_i\} \tag{23}$$

where

$$\{B'_i\} = \{B_i\} - [A_{kj}{}^w]\{\Delta\phi_{wk}\} \tag{24}$$

The velocity potential ϕ is then given by

$$\{\phi_s\} = [C_{ij}]\{\sigma_j\} + [C_{ik}{}^{ws}]\{\Delta\phi_{wk}\} \tag{25}$$

and

$$\{\phi_{wm}\} = [C_{ij}{}^{sw}]\{\sigma_j\} + [C_{ik}{}^{ww}]\{\Delta\phi_{wk}\} \tag{26}$$

where

$$C_{ij} = \frac{1}{4\pi}\iint_{\text{el } i}\frac{\sigma(\xi,t)}{\sigma(\mathbf{x}_{oi},t)}\,\frac{\partial}{\partial \nu(\xi,t)}\left[\frac{1}{R(\mathbf{x},\xi,t)}\right]dS \tag{27}$$

Combining Eqs. (23) and (25), the potential operator employed in the preceding section can be defined. Hence

$$\phi(\mathbf{x}_j,t) = PO\big(\{B(\mathbf{x}_i,t)\} - [A_{kj}{}^w]\{\Delta\phi_{wk}\}\big) + [C_{kj}{}^w]\{\Delta\phi_{wk}\} \tag{28}$$

which reduces to (14) in the absence of the wake.

To evaluate the integrals (21) and (27), three processes are involved. These are the simplification of the geometry of the surface elements and the proper selection of the doublet distribution function, both for the purpose of analytically evaluating these integrals and efficient computation, and a suitable choice of control and source points required for best accuracy. The source point is defined as a representative point at a surface element, at which the value of the doublet distribution is sought, and a control point is defined as a point at which the flow tangency condition is to be satisfied. In some methods, these sets of points belong to a single set, generally referred as the collocation points, whereas in other methods, distinct sets of points are utilized, such as the familiar set in lifting line theory, in which the vortex line is specified on the quarter-chord points and the downwash velocities are evaluated at the three-quarter-chord points. Since the kernel functions of the integrals (21) and (27) are singular, care should be exercised in the selection of the doublet distribution functions and the control and source points.

One possible way to simplify the geometry of the surface elements is to employ planar quadrilaterals, using a procedure essentially similar to that of Ref. 14. The characteristic dimension of such an approximate element should be much smaller than the local radius of curvature of the original surface element. Figure 1b illustrates a typical arrangement of surface elements. Further approximation by rectangular surface elements may also be possible, and is in fact desirable in view of its symmetrical properties and simplified analytical evaluation of the integrals (21) and (27).

Systematic Expansion of the Velocity Influence Coefficient

To choose a proper doublet distribution function over each of the surface elements, attention is focused on the far-field and near-field behavior of the velocity influence coefficient and means for efficient, yet accurate, simplification.

A formal analysis can be performed by Taylor series expansion of σ and the velocity kernel function $[\partial^2/\partial n(\mathbf{x},t)\partial \nu(\xi,t)][1/R(\mathbf{x},\xi,t)]$. Hence

$$\sigma(\mathbf{x}) = (0) + x\left.\frac{\partial \sigma}{\partial x}\right|_{\mathbf{x}=0} + y\left.\frac{\partial \sigma}{\partial y}\right|_{\mathbf{x}=0} + \frac{1}{2}x^2\left.\frac{\partial^2}{\partial x^2}\right|_{\mathbf{x}=0} + \frac{1}{2}y\left.\frac{\partial^2 \sigma}{\partial y^2}\right|_{\mathbf{x}=0} + xy\left.\frac{\partial^2}{\partial x \partial y}\right|_{\mathbf{x}=0} + \ldots \tag{29}$$

and

$$K_v(\mathbf{x},\xi,t) = K_v(\mathbf{x},\mathbf{0},t) + xK_{v_x}|_{\mathbf{x}=\mathbf{0}} + yK_{v_y}|_{\mathbf{x}=\mathbf{0}} + \tfrac{1}{2}x^2K_{v_{xx}}|_{\mathbf{x}=\mathbf{0}} + \tfrac{1}{2}y^2K_{v_{yy}}|_{\mathbf{x}=\mathbf{0}} + xyK_{v_{xy}}|_{\mathbf{x}=\mathbf{0}} + \ldots \quad (30)$$

Here we have employed an element coordinate system with its origin at the source point of the surface element being considered. For a field point in the far field, substituting (29) and (30) into (21) and retaining terms up to the second order yields the following expression:

$$A_{ij} = (A/4\pi)[\{1 + \bar{\sigma}_x M_x/A + \bar{\sigma}_y M_y/A + \tfrac{1}{2}\bar{\sigma}_{xx}I_{xx}/A + \bar{\sigma}_{xy}I_{xy}/A + \tfrac{1}{2}\bar{\sigma}_{yy}I_{yy}/A\}K + K_x\{M_x/A + \bar{\sigma}_x I_{xx}/A\} + K_y\{M_y/A + \bar{\sigma}I_{yy}/A\} + \tfrac{1}{2}K_{xx}I_{xx}/A + K_{xy}I_{xy}/A + \tfrac{1}{2}K_{yy}I_{yy}/A + \ldots] \quad (31)$$

At the centroid of the surface element, $M_x = M_y = 0 = I_{xy}$, and to a second-order accuracy, we could set $A_{ij} = AK_v(\mathbf{x},\mathbf{0},t)/4\pi$. It is then suitable to locate the source point at the centroid of the surface element. Expression (31), in addition, can be interpreted as a multipole expansion, since the coefficients of K_{v_x} and K_{v_y} represent the strengths of quadrupoles at the source point, whereas the coefficients of $K_{v_{xx}}$ and $K_{v_{yy}}$ are octupoles, with appropriate orientations. The use of (31) or its approximation is dictated by the accuracy, as compared to a more exact formula derived for the near-field region. For the near-field region, we would employ (29) and then perform the integration (21) analytically.

Since additional unknowns represented by the derivatives of σ are introduced in the process of matrix inversion (23), resort is made to a finite-difference version, so that these derivatives are expressed in terms of σ_i's. For most applications, we could disregard the variation of σ along one coordinate, so that in general we could write Eq. (19) as

$$\sigma(\mathbf{x}) = \sigma(\mathbf{0})(a + bx + cx^2 + \ldots) \quad (32)$$

and hence

$$A_{ij} = \frac{1}{4\pi}\iint_{\text{el}\,i}(a + bx + cx^2 + \ldots)K_v(\mathbf{x}_j,\mathbf{x},t)dS \quad (33)$$

Since $K_v(\mathbf{x}_j,\mathbf{x},t)$ is a singular function of the fifth power, the velocity influence integral (33) is singular for field points located in a region for which the doublet distribution function (32) or its slope (x-derivative) possesses a discontinuity in that region.[16] Obviously a control point should not be located at this region, and to avoid any such region, one has to represent the doublet distribution by a function that possesses no discontinuity up to its slope. In view of this argument, representation of σ by a function of order higher than two is not necessary. This argument is valid for representation of σ as a function of a single variable.

Before proceeding to the three-dimensional problems, much could be gained from a study of the two-dimensional situations. Consider three finite-difference approximations of σ based on (32), written in general forms as

1) $\sigma(\mathbf{x}) = \alpha$ (step distribution, zeroth-order approximation)

2) $\sigma(\mathbf{x}) = \alpha + \beta x$ (piecewise linear distribution, first-order approximation)

3) $\sigma(\mathbf{x}) = \alpha + \beta x + \gamma x^2$ (piecewise quadratic distribution, second-order approximation

where α, β, and γ are coefficients numerically determined by finite-difference analysis and dependent on the values of σ_i's in the neighborhood of each source point in question. These distributions are illustrated in Fig. 2. The control points for the first and third distributions are located at the source points. For no discontinuity in the slope of σ, this would result in the minimization of error, as can be verified by treating the near-field behavior in a way similar to that employed in the choice of the source point.[16] The piecewise linear distribution can be regarded as a superposition of elementary triangular distributions, as shown in Fig. 2. Since the vertices are points of slope discontinuity, and by locating the control point midway between the vertices unequal number of source and control points result (except for the steady-state case by imposing the Kutta-Joukowski condition at the trailing edge), the use of a piecewise linear distribution does not seem plausible and will not be considered further in the three-dimensional case.

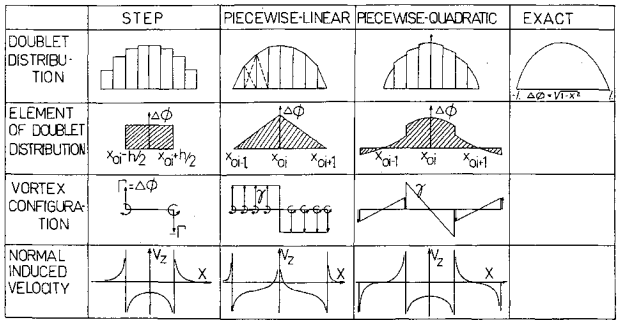

Fig. 2 Approximate doublet distribution functions.

The piecewise quadratic distribution is of interest. Such a distribution can be represented, between a region bounded by $x_{oi} - \frac{1}{2}h$ and $x_{oi} + \frac{1}{2}h$, by

$$\sigma = \frac{(x - x_{oi})(x - x_{oi+1})}{(x_{oi-1} - x_{oi})(x_{oi-1} - x_{oi+1})}\sigma_{i-1} + \frac{(x - x_{oi-1})(x - x_{oi+1})}{(x_{oi} - x_{oi-1}) - (x_{oi} - x_{oi+1})}\sigma_i + \frac{(x - x_{oi-1})(x - x_{oi})}{(x_{oi+1} - x_{oi-1})(x_{oi+k} - x_{oi})}\sigma_{i+1} \quad (34)$$

Consequently, this type of approximate distribution would still be discontinuous at the edges of each element, but for each element, variation of the doublet distribution over the element up to its second order has been taken into account. Carrying out the integration of the velocity influence coefficient and substituting into expression (20), and rearranging, we obtain

$$\sum_{i=1}^{N}\Delta\phi_i(A_{ij}{}^o + A_{i+1,j}{}^r + A_{i-1,j}{}^l) = B'_j \quad (35)$$

where

$$A_{ij}{}^o = \frac{1}{2\pi}\int_{\text{el}\,i}\frac{(x - x_{oi+1})(x - x_{oi-1})}{(x_{oi} - x_{oi+1})(x_{oi} - x_{oi-1})}K_{v2}(x,x_j)dx \quad (36)$$

$$A_{i+1,j}{}^r = \frac{1}{2\pi}\int_{\text{el}\;i+1}\frac{(x - x_{oi+1})(x - x_{oi+2})}{(x_{oi} - x_{oi+1})(x_{oi} - x_{oi+2})}K_{v2}(x,x_j)dx \quad (37)$$

$$A_{i-1,j}{}^l = \frac{1}{2\pi}\int_{\text{el}\;i-1}\frac{(x - x_{oi-1})(x - x_{oi-2})}{(x_{oi} - x_{oi-1})(x_{oi} - x_{oi-2})}K_{v2}(x,x_j)dx \quad (38)$$

$$K_{v2}(x,x_j) = \frac{[(x - x_j)^2 - z_j{}^2]n_{z_j} - 2z_j(x - x_j)n_{x_j}}{[(x - x_j)^2 + z_j{}^2]^2} \quad (39)$$

which can readily be evaluated. $A_{ij}{}^o$ corresponds to the doublet distribution extending within the element i, whereas $A_{i+1,j}{}^r$ and $A_{i-1,j}{}^l$ are contributed by the parts of the element of the doublet distribution associated with the source element i which extend on the right-hand side and the left-hand side, respectively, as illustrated in the fourth column, second row of Fig. 2.

In the three-dimensional situation, we would consider planar quadrilateral and rectangular surface elements. For a rectangular surface element characterized by the sides D_1 and D_2, the velocity influence coefficient normal to the surface

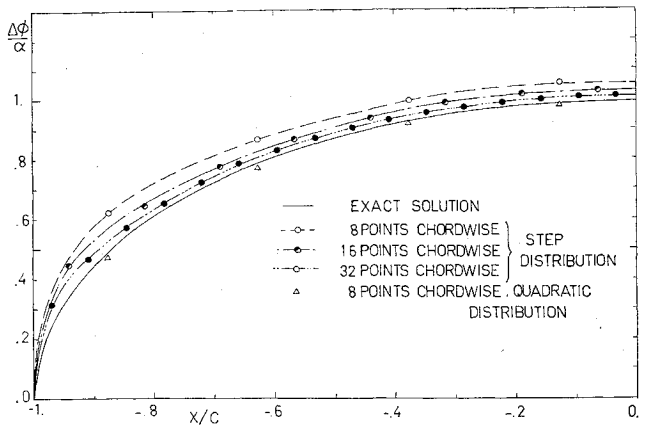

Fig. 3 Two-dimensional chordwise distribution of doublet at the instant of starting.

element of the control point, for a step distribution, is given by

$$A_{ij} = -n_{zj}A_{1ij} - 3n_{xj}A_{2ij} - 3n_{yj}A_{3ij} \tag{40}$$

where

$$A_{1ij} = \frac{1}{4\pi}\int_{-D_{1i}/2}^{D_{1i}/2}\int_{-D_{2i}/2}^{D_{2i}/2}\left[\frac{3z_j^2}{[(x-x_j)^2+(y-y_j)^2+z_j^2]^{5/2}} - \frac{1}{[(x-x_j)^2+(y-y_j)^2+z_j^2]^{3/2}}\right]dxdy \tag{41}$$

$$A_{2ij} = \frac{1}{4\pi}\int_{-D_{1i}/2}^{D_{1i}/2}\int_{-D_{2i}/2}^{D_{2i}/2}\frac{(y_j-y)z_j}{[(x-x_j)^2+(y-y_j)^2+z_j^2]^{5/2}}\times dxdy \tag{42}$$

$$A_{3ij} = \frac{1}{4\pi}\int_{-D_{1i}/2}^{D_{1i}/2}\int_{-D_{2i}/2}^{D_{2i}/2}\frac{(x_j-x)z_j}{[(x-x_j)^2+(y-y_j)^2+z_j^2]^{5/2}}\times dxdy \tag{43}$$

Each of these terms represents the induced velocity in the z, x, and y direction, respectively, of the surface element i. The step distribution is equivalent to the vortex lattice of rectangular shape (or of the shape of the polygonal surface element), and by the use of Biot-Savart law, Eq. (40) could again be obtained. For $R/D > 2.5$, where D is the largest of D_1 and D_2, a multipole expansion approximate formula has proved to give sufficient accuracy. Since the expression for the influence coefficient associated with the piecewise quadratic distribution, which was chosen to take place along the chordwise direction, is lengthy, it will not be reproduced here. Detailed description is outlined in Ref. 16.

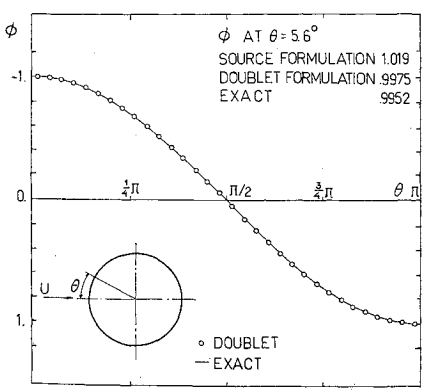

Fig. 4 Velocity potential distribution over the surface of a cylinder in nonlifting potential flow.

IV. Application

Application to the Starting Instant Problem

Figure 3 displays the doublet distribution over a flat plate of infinite aspect ratio, obtained by employing step and piecewise quadratic distribution functions. The spacing between the elements is uniform. The step doublet distribution approximation predicts a doublet distribution that overestimates the exact one; for 32 elements, an agreement within 3% is indicated, but agreement becomes worse near the leading and trailing edges. Convergence of the solution can be observed with the increase of the number of elements, but near the edges, increase of the number of elements alone is not sufficient, since $\Delta\phi$ varies rapidly there. Although variable spacing to allow denser elements at regions of rapidly varying doublet distribution would improve the accuracy, the use of a more accurate representation at the edges would result in best accuracy. Rapid convergence (in the sense of a small number of elements) could be obtained by the use of a piecewise quadratic distribution. For 8 elements an agreement within 1% is indicated, but the result underestimates the exact distribution. Such a behavior can be verified to be a consequence of the behavior of the self-induced velocity influence coefficient, which dominates the induced downwash at any field point.

Another point of interest is the ability of the doublet scheme to deal with the thickness problem. For this purpose, the method is applied to the nonlifting flow around a circular cylinder. The result indicates an excellent agreement with the exact solution, i.e., 0.5% for 64 elements, as shown in Fig. 4.

Figure 5a displays the doublet distribution over an elliptical planform using step and piecewise quadratic doublet distribution functions. Rectangular elements were employed, and care is taken to obtain proper representation of the tip sections. Again, better convergence is indicated by the piecewise quadratic distribution approximation. In these calculations, only 16 elements arranged as a network of 4 by

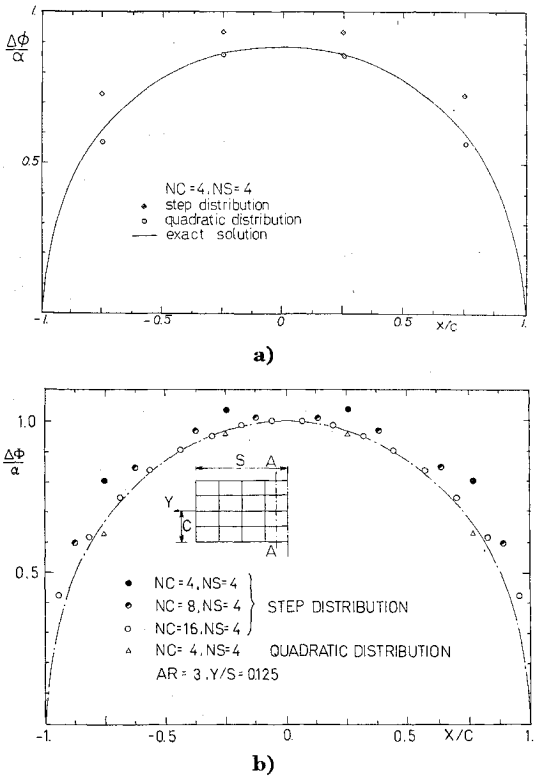

Fig. 5 Chordwise doublet distribution for a finite planform at the starting instant, AR = 3, at midspan section; a) elliptical planform, b) rectangular planform.

4 were used. The agreement with the exact solution is fair for the step distribution.

To investigate the convergence behavior, the method is applied to a rectangular planform, for which no surface element approximation is necessary. The results shown in Fig. 5b indicate a converging behavior for the step distribution approximation with 64 elements arranged as a 16 by 4 network and for a piecewise quadratic distribution approximation with a 4 by 4 network. Although better convergence seems to be indicated by the use of a piecewise quadratic distribution approximation, in further application, the choice between the two distributions would be dictated by the computation time required for a comparable accuracy. A separate study to optimize the computation is necessary. Nevertheless, the step distribution has given a reasonably good prediction, except for the tip regions, for which the inaccuracy would be of a local nature. Improvement of the accuracy can be made by incorporating a better (higher-order) approximation, as before, or by employing more elements at this region. The results just described lend support to the application of the method to the more complicated problems which involve the unsteady deforming wake.

Application to Impulsively Started Planforms and Comparison of Results

The transient loading on a wing impulsively started with a uniform velocity $U = U_o$ will be considered. To compare the accuracy provided by the present method, two-dimensional cases are first considered. Figure 6 exhibits the indicial circulation experienced by a two-dimensional flat plate. Comparison is made with the prediction of R. T. Jones,[22] which is based on a linearized formulation of the problem. In particular, Jones' calculation is based on operational methods to solve two integral equations simultaneously; the first equation relates the induced downwash to the circulation of the airfoil along a straight path, and the second is an integral equation relating the circulation along the flight path to the rise of circulation following a sudden start of motion. The present computation incorporates a step doublet distribution over each element. In the linear region, say $\alpha = 0.1$ rad, the agreement is excellent. Similarly, the indicial lift (Wagner function) compares very well with standard result[23] for a small angle of attack. The computation of lift was based on the superposition of the steady part according to the alternate method discussed in Sec. II and the numerical integration of the unsteady pressure coefficient over the surface S. These two parts are both circulatory, except at the starting instant, for which the latter term is the added mass. Several time steps were employed, the results indicating satisfactory convergence for $\Delta tU/(\frac{1}{2}c) = 0.125$ or less; the time step is commensurate with the spacing of the elements along the chord. The nonlinearities introduced by the wake geometry can be observed from Fig. 7a. Calculation of the wake trajectory is obtained by incorporating the method to evaluate Eqs. (17) and (18) numerically, which may involve the use of a predictor-corrector scheme[7,16] for improved accuracy. Three wake geometries were considered, as depicted in Fig. 7b, namely a freestream directed wake, a straight wake tangent to the limiting streamline at the trailing edge, and a field-induced deforming wake with rolled up starting vortex. For an angle of incidence of 0.3 rad, the indicial circulation associated with these wake configurations differ within 4% at s, the distance travelled by the airfoil, equal to 1.25. As s increases, the indicial circulation for the field-induced deformed wake approaches that of the freestream directed wake.

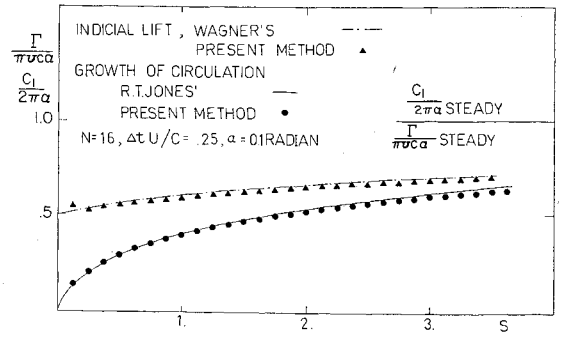

Fig. 6 Indicial lift and growth of circulation for an impulsively started two-dimensional flat plate.

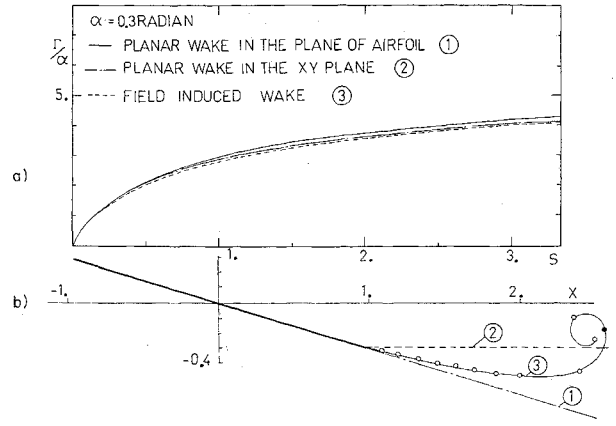

Fig. 7 Effect of the wake geometry on the growth of circulation of an impulsively started flat plate (2 dimensions).

To illustrate the capabilities of the present method, Fig. 8 shows the Küssner function (due to Von Kármán and Sears[21]) predicted by the present method for a gust onset velocity equal to 0.1 U_o striking a two-dimensional flat plate. Figure 9 indicates the wake pattern behind an impulsively started, oscillating flat plate that exhibits a qualitative similarity with the visual observation of Bratt[24] for a steady-state oscillation and Giesing's calculation[7] for a similar transient oscillation.

The indicial sectional circulations for rectangular and elliptical planforms are shown in Figs. 10a and 10b, and comparision is made to the two-dimensional result. The more significant indicial lift function for a rectangular planform of aspect ratio 6 is shown in Fig. 10c, and exhibits an excellent agreement with the linearized theory of W. P. Jones,[25] for a small angle of incidence. These results again serve to verify the feasibility of the present method.

The effects of the aspect ratio and the geometry of the planform on the indicial loading can be studied from these results. The dependency on the angle of incidence is shown in Fig. 11, where the method has been applied to a rectangular planform of aspect ratio 6; the effect of thickness can be observed from Fig. 12, for rectangular planforms with NACA profiles of thickness ratios 0.12 and 0.15. Similar behavior is also given by Giesing.[7]

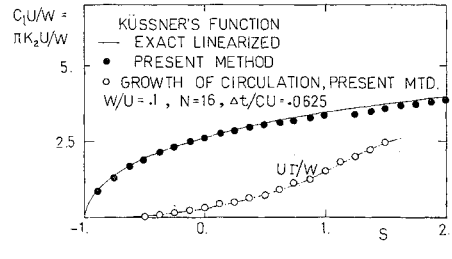

Fig. 8 Indicial lift and growth of circulation for a two-dimensional flat plate entering a sharp-edged gust.

a) Visual Study by Bratt - Steady State Oscillation

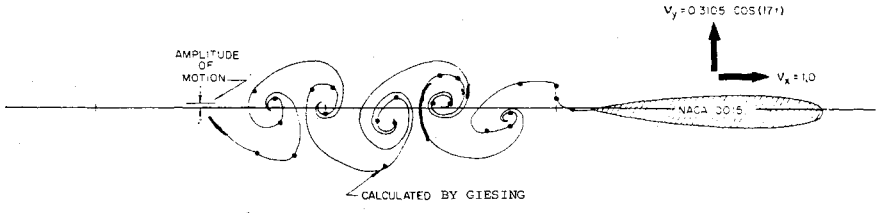

b) Giesing's Calculation - Transient Oscillation

Fig. 9 Wake pattern behind an oscillating foil.

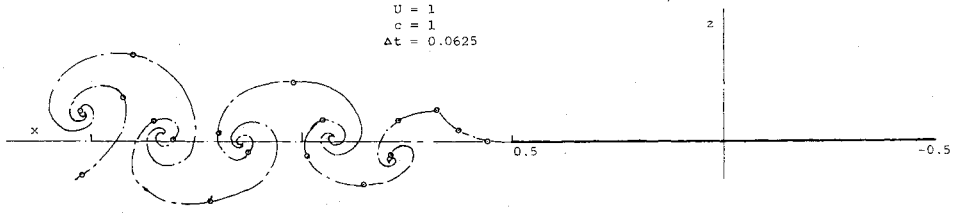

c) Calculated using present method for a two-dimensional flat plate - transient oscillation

V. Conclusions

A numerical method has been developed which has been demonstrated in its potentialities to solve nonlinear transient lifting potential flow problems for wings of arbitrary planforms with thickness, although for comparison only simple planforms were considered. Employing a finite-difference version of the Taylor series expansion, it has been shown that step doublet distribution is sufficient to predict accurate airloads, and improvement of the accuracy is also suggested according to the framework of the method outlined herein.

In particular, the present method finds its usefulness in accounting for the thickness effects and moderate angle of incidences beyond the range of linear theory. In addition, it is possible to predict the location of the unsteady and deforming wake. Near the wing tip regions, however, the effects of the wake at the present moment should be interpreted with reservation, since the influence of the rolling up of the tip vortex, which becomes more significant at higher angle of incidences and smaller aspect ratios, should be carefully taken into account. In the present exploratory calculations, the grid was too coarse in the spanwise direction near the tip to properly account for the details of tip vortex rollup. In addition, viscous effects in a tip vortex core should be included in any such calculation.

The present method provides a basis for a more careful treatment of more difficult problems, such as bodies in ground effects, the interaction between a wing and a returning wake, and unsteady problems with aeroelastic effects. To treat periodic motion, one could either proceed as before along the step-by-step calculation, until all transient effects subside,

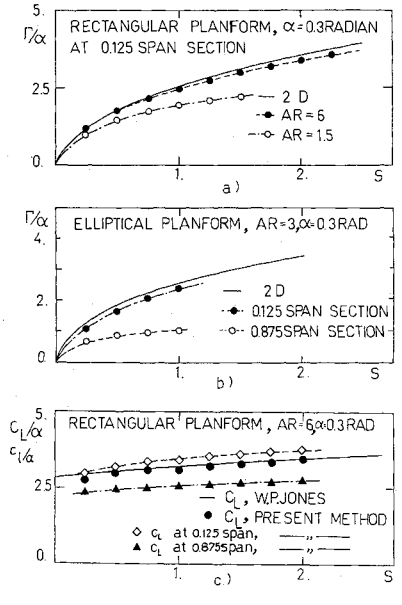

Fig. 10 Indicial loading of an impulsively started finite planform; a) growth of circulation for a rectangular planform, b) growth of circulation for an elliptical planform, c) indicial lift for a rectangular planform.

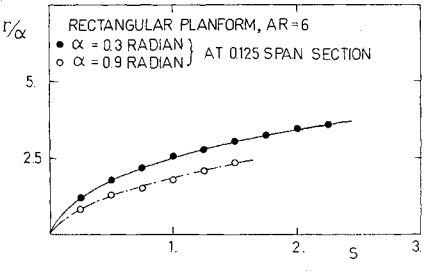

Fig. 11 Growth of circulation for an impulsively started rectangular planform at various angles of incidence.

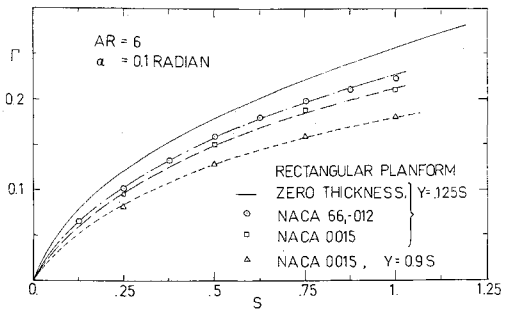

Fig. 12 Growth of circulation of an impulsively started thick wing of rectangular planform and NACA profile.

or employ some modification which includes an initially assumed wake.

References

[1] Greidanus, J. H., van de Vooren, A. I., and Bergh, H., "Experimental Determination of the Aerodynamic Coefficients of an Oscillating Wing in Incompressible Two-Dimensional Flow," Repts. F-101 to F-104, 1952, National Luchtvaart Laboratorium.

[2] Ransleben, G. E., Jr. and Abramson, H. N., "Experimental Determination of Oscillatory Lift and Moment Distributions of Fully Submerged Flexible Hydrofoils," Rept. 2, Contract Nonr-3335 (00), 1962, Southwest Research Institute, San Antonio, Texas.

[3] Spurck, J., "Messungen der Aerodynamischen Beiwerte Schwingender Flugelprofil in Windkanal und Vergleich met der Theorie," NR. 29, 1963, Mitteilungen Max-Planck Institute, Gottingen.

[4] Küssner, H. G. and von Gorup, G., "Instationäre Lineasierte Theorie der Flugelprofile endlicher Dicke in Inkompressibler Stromung," NR. 26, 1960, Mitteilungen Max-Planck Institute, Gottingen.

[5] van de Vooren, A. I. and van de Vel, H., "Unsteady Profile Theory in Incompressible Flow," Rept. TW-17, 1963, Mathematics Institute, Rijksuniversiteit, Groningen, The Netherlands.

[6] Hewson-Browne, R. C., "The Oscillation of a Thick Aerofoil in an Incompressible Flow," *Quarterly Journal of Mechanics and Applied Mathematics*, Vol. 16, 1963, pp. 79–92.

[7] Giesing, J. P., "Nonlinear Two-Dimensional Unsteady Potential Flow with Lift," *Journal of Aircraft*, Vol. 5, No. 2, March-April 1968, pp. 135–143.

[8] Chen, C. F. and Wirtz, R. A., "Second-Order Theory for Flow Past Oscillating Foils," *AIAA Journal*, Vol. 6, No. 8, Aug. 1968, pp. 1556–1562.

[9] Ashley, H., Widnall, S. E., and Landahl, M. T., "New Directions in Lifting Surface Theory," *AIAA Journal*, Vol. 3, No. 1, Jan. 1965, pp. 3–15.

[10] Landahl, M. T. and Stark, V. J. E., "Numerical Lifting Surface Theory—Problems and Progress," AIAA Paper 68-72, New York, 1968.

[11] Miller, R. H., "Rotor Blade Harmonic Loading," *AIAA Journal*, Vol. 2, No. 7, July 1964, pp. 1254–1269.

[12] Miller, R. H., "Unsteady Air Loads on Helicopter Rotor Blades," *Journal of the Royal Aeronautical Society*, Vol. 68, April 1964, p. 640.

[13] Ashley, H., "Machine Computation of Aerodynamic Loads in Linear and Nonlinear Situations," Rept. 66-5, AFOSR 66-1440, Fluid Dynamics Research Lab., Massachusetts Institute of Technology.

[14] Hess, J. L. and Smith, A. M. O., "Calculation of Potential Flow About Arbitrary Bodies," *Progress in Aeronautical Sciences*, Vol. 8, Pergamon, New York, 1966.

[15] Rubbert, P. E. et al., "A General Method for Determining the Aerodynamic Characteristics of Fan-in-Wing Configuration," TR 67-61A, 1967, U. S. Army Aviation Materiel Lab.

[16] Djojodihardjo, R. H., "A Numerical Method for the Calculation of Nonlinear Unsteady Lifting Potential Flow Problems," Sc.D. thesis, Feb. 1969, Dept. of Aeronautics and Astronautics, Massachusetts Institute of Technology.

[17] Hadamard, J., "The Finite Part of an Infinite Simple Integral," *Lectures on Cauchy's Problem in Linear Partial Differential Equations*, Dover, New York, 1952, pp. 133–141.

[18] Mangler, K. W., "Improper Integrals in Theoretical Aerodynamics," C.P. 94, 1952, Aeronautical Research Council, Great Britain.

[19] Thwaites, B., *Incompressible Aerodynamics*, Macmillan, New York, 1960.

[20] Wagner, H., "Uber die Entstehung des Dynamischen Auftriebes von Traflugeln," *Zeitscrift fur Angewandte Mathematik und Mechanik*, Vol. 5, No. 1, Feb. 1925.

[21] von Kármán, T. and Sears, W. R., "Airfoil Theory for Nonuniform Motion," *Journal of the Aeronautical Sciences*, Vol. 5, No. 10, Aug. 1938, pp. 379–390.

[22] Jones, R. T., "The Unsteady Lift of a Finite Wing," TN 682, 1939, NACA.

[23] Garrick, I. E., "Nonsteady Wing Characteristics," *High Speed Aerodynamics and Jet Propulsion*, Vol. VII, Princeton University Press, Princeton, N. J., 1957, Sec. F.

[24] Bratt, J. B., "Flow Patterns in the Wake of Oscillating Airfoil," R & M 2773, 1953, Royal Aeronautical Establishment, Great Britain.

[25] Jones, W. P., "Aerodynamic Forces on Wings in Nonuniform Motion," R & M 2117, 1945, Aeronautical Research Council, Great Britain.